Influences of spark plasma sintering temperature on the microstructures and thermoelectric properties of $(Sr_{0.95}Gd_{0.05})TiO_3$ ceramics*

Li Liang-Liang(李亮亮)[a)b)†], Qin Xiao-Ying(秦晓英)[c)], Liu Yong-Fei(刘永飞)[c)], and Liu Quan-Zhen(刘全桢)[a)b)]

[a)] *SINOPEC Research Institute of Safety Engineering, Qingdao* 266071, *China*
[b)] *State Key Laboratory of Chemical Safety, Qingdao* 266071, *China*
[c)] *Key Laboratory of Materials Physics, Institute of Solid State Physics, Chinese Academy of Sciences, Hefei* 230031, *China*

(Received 5 January 2015; revised manuscript received 21 January 2015; published online 10 April 2015)

$(Sr_{0.95}Gd_{0.05})TiO_3$ (SGTO) ceramics are successfully prepared via spark plasma sintering (SPS) respectively at 1548, 1648, and 1748 K by using submicron-sized SGTO powders synthesized from a sol–gel method. The densities, microstructures, and thermoelectric properties of the SGTO ceramics are studied. Though the Seebeck coefficient shows no obvious difference in the case that SPS temperatures range from 1548 K to 1648 K, the electrical conductivity and the thermal conductivity increase remarkably due to the increase in grain size and density. The sample has a density higher than 98% theoretical density as the sintering temperature increases up to 1648 K and shows average grain sizes increasing from ~ 0.7 μm to 7 μm until 1748 K. As a result, the maximum of the dimensionless figure of merit of ~ 0.24 is achieved at ~ 1000 K for the samples sintered at 1648 K and 1748 K, which was $\sim 71\%$ larger than that (0.14 at ~ 1000 K) for the sample sintered at 1548 K due to the enhancement of the power factor.

Keywords: sintering, transitional metal oxides, ceramics, thermoelectric properties

PACS: 72.20.Pa, 72.80.Ga, 73.50.Lw **DOI:** 10.1088/1674-1056/24/6/067202

1. Introduction

Over the past two decades, thermoelectric (TE) materials have attracted a great deal of attention due to their potential applications in heat-to-electricity conversion.[1] The energy conversion efficiency of a TE material is usually characterized by the dimensionless figure of merit (ZT), defined as $ZT = S^2\sigma T/\kappa$, where S is the Seebeck coefficient, T is the absolute temperature, σ is the electrical conductivity, and κ is the total thermal conductivity. Heavy metallic alloys such as Bi_2Te_3, PbTe, and other relevant materials possess high thermoelectric performances ($ZT =\sim 1$) at low temperature.[2,3] However, the high-temperature instability and toxicity of these materials restrict the practical applications at high temperature. Therefore, oxide materials, composed of non-toxic, naturally abundant and low cost elements with high stability, are promising for extensive applications in TE devices at elevated temperature.[4,5]

The ZT values of n-type bulk oxides are lower than those of the p-type oxides, which limits the harvest of electric energy via the p-type and n-type thermoelectric circuits. Among possible alternating materials, donor-doped $SrTiO_3$ (STO) has been considered as a promising n-type TE oxide in the high temperature range.[6] However, the conventional fabrication method based on the solid-state reaction (SSR) requires intermediate heat treatments in air at high temperature several times due to the low cation diffusion coefficients in oxides, which is quite energy-consuming.[7,8] On the other hand, a high-temperature-processed oxide will give rise to large grain size, which is detrimental to enhancing the phonon scattering.[9] In order to obtain homogeneous powders with uniform particle size distribution, several alternatives based on wet chemical routes have been used to prepare pure STO and donor-doped STO.[10] Recently, a combination of sol–gel process and spark plasma sintering (SPS) was introduced on account of the molecular-scale mixing of cations and the rapid densification, which was of benefit to fabricating highly dense compounds with ultra-fine grain sizes in a short time.[11] Nevertheless, it has been revealed that though the κ was reduced to 1.19 W/mK at 773 K in the La-doped STO due to the fine grains (~ 300 nm), a smaller ZT value (< 0.02 at 773 K) was obtained due to the poor electrical conductivity.[11] This problem should be solved synthetically by introducing more donor-type oxygen vacancies in reducing atmosphere and/or sintering at elevated temperature (to provide additional itinerant carriers to the conduction band),[12] and improving the densification to suppress the strong charge carrier scattering at the pore sites (to elevate PF).[13] In this study, submicron-sized $(Sr_{0.95}Gd_{0.05})TiO_3$ (SGTO) powders are first synthesized by a sol–gel method, and then dense SGTO ceramics are prepared by SPS using pre-annealed SGTO in reducing atmosphere. The morphologies and microstructures of the SGTO powders and ceramics are characterized, and the influence of sintering

*Project supported by the National Natural Science Foundation of China (Grant Nos. 11174292, 51101150, and 11374306).
†Corresponding author. E-mail: lgli@mail.ustc.edu.cn
© 2015 Chinese Physical Society and IOP Publishing Ltd

temperature on the TE properties is also discussed.

2. Experimental procedure

2.1. Materials

Strontium nitrate ($Sr(NO_3)_2$, $\geq$ 99.5%), gadolinium (III) nitrate hexahydrate ($Gd(NO_3)_3{\cdot}6H_2O$, $\geq$ 99.9%), citric acid monohydrated (CA, $\geq$ 99.5%), tetrabutyl titanate (AR), alcohol (AR), and ethylene glycol (AR) were obtained from Sinopharm Chemical Reagent Co., Ltd (China), and directly used without further purification.

2.2. Preparation of SGTO powders

Powders of SGTO were synthesized by the sol–gel process. Firstly, the $Sr(NO_3)_2$, $Gd(NO_3)_3{\cdot}6H_2O$, and CA were dissolved into the deionized water. Secondly, an appropriate amount of tetrabutyl titanate was mixed with alcohol and ethylene glycol in the 1:20:1 molar ratio, and the mixture was slowly dropped into the above solution with continuous stirring at 343 K until a viscous sol was formed (Sr:Gd:Ti in the desired ratios, and the total metal cations:CA molar ratio = 1:3). Thirdly, the sol was aged at 353 K for 24 h, then dried at 453 K for 6 h to promote polymerization and a xerogel was obtained. Finally, the SGTO powders were produced by calcinating the xerogel at 1223 K for 6 h in air.

2.3. Preparation of SGTO ceramics

The synthesized SGTO powders were annealed at 1473 K for 2 h in forming gas of 5 vol% hydrogen in argon. After intermediate grinding, ceramic samples were sintered by SPS under 40 MPa for 10 min in an Ar flow. In this study, the samples were spark-plasma-sintered (SPSed) at 1548, 1648, and 1748 K, respectively, with a heating rate of 100 K/min. The corresponding samples, for the sake of simplifying description, were referred to as S1548, S1648, and S1748, respectively.

2.4. Characterization

The phase identifications of the samples were investigated by x-ray diffraction (XRD) using a Cu $K\alpha$ irradiation (Philips X'pert) and the morphologies were examined by field emission scanning electron microscopy (FESEM, Sirion 200 FEI). The values of σ and S for the samples were measured simultaneously using a ZEM-3 equipment (Ulvac Riko, Inc.) in helium atmosphere. The values of thermal diffusivity (D) and specific capacity (C_p) were measured by a laser-flash method (Netzsch, LFA 457) and differential scanning calorimetry (DSC, Perkin–Elmer), respectively. The values of density (λ) were measured by the Archimedes' method and the total thermal conductivity κ was calculated from the formula $\kappa = DC_p\lambda$.

3. Results and discussion

Figure 1 shows the XRD patterns of xerogel and SGTO powders calcined at 1223 K. An amorphous phase is obtained for the xerogel. The crystalline phase of the SGTO powders is identified as $SrTiO_3$, and all of the diffraction peaks for the SGTO powders could be indexed as cubic STO (JCPDS No. 35-0734). For the conventional ceramic processing of donor-doped $SrTiO_3$, an intermediated heat treatment in air at $T \geq 1473$ K for several hours was generally required to obtain a well-crystallized STO phase.[7,8] Hence, one can see that the synthesis temperature could be reduced distinctly in this sol–gel process, which should be caused by the short-range diffusion path of the element during sol–gel formation.

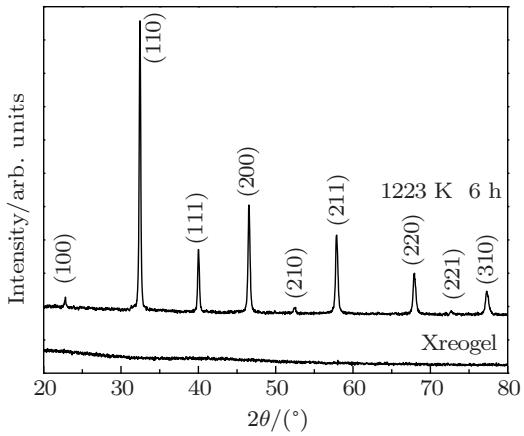


Fig. 1. XRD patterns of xerogel and SGTO powders calcined at 1223 K.

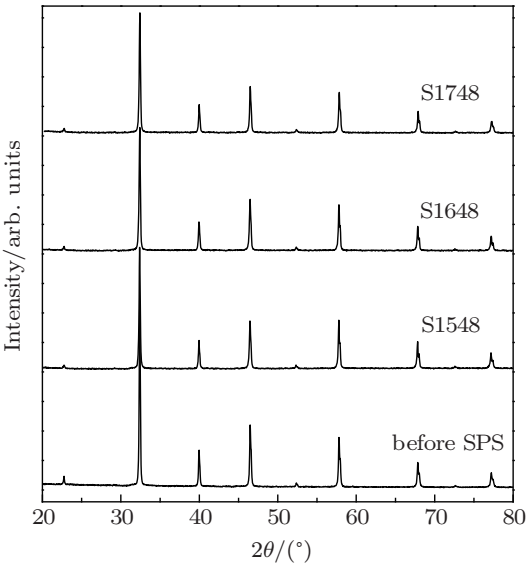


Fig. 2. XRD patterns of SGTO powders annealed at 1473 K (before SPS) and SGTO ceramics SPSed at 1548 K (S1548), 1648 K (S1648), and 1748 K (S1748) respectively.

Room-temperature XRD patterns of the SGTO powders annealed at 1473 K (before SPS) and SGTO ceramics SPSed at different temperatures are shown in Fig. 2. All of the samples are completely indentified as having a cubic perovskite-type structure, without any detectable impurity peaks, indicating

that no phase transformation occurs in the powder reduction process nor in the high temperature sintering process. The lattice parameter a (3.9030 Å) of the SGTO powder before SPS is calculated from the XRD patterns by using an Si standard for calibration. The theoretical density (TD $\sim$ 5.22 g/cm^3) of the ceramic is estimated from the calculated lattice constant, and the variation of the lattice constant originates from the formation of oxygen deficiencies for the sintered SGTO ceramics and is neglected. The densities for samples S1548, S1648, and S1748 are 4.95, 5.15, and 5.14 g/cm^3 respectively. The relative density is defined as the measured density over the theoretical density. One can see that the relative densities are about 94.8%, 98.7%, and 98.5% for the samples S1548, S1648, and S1748, respectively.

Figure 3 shows the FESEM images of the annealed SGTO powders, the mirror-polished and thermal etched surfaces of all the SGTO samples. The particle sizes of the SGTO powders are less than 500 nm (Fig. 3(a)). The submicron-sized particles would give rise to a promoting driven force for sintering and densification,[14] which results in a reduced densification temperature compared with the SSR ($T > 1700$ K).[8] As mentioned above, the sample SPSed at 1648 K (98.7% TD) has a higher relative density than the (94.8% TD) SPSed at 1548 K with the same duration time, indicating a high densification rate at 1648 K. In view of the relationship between the densification rate ($\mathrm{d}\rho/\rho\,\mathrm{d}t$, where ρ is the relative density and t is the time) and grain boundary diffusivity (D_b): $\mathrm{d}\rho/\rho\,\mathrm{d}t \propto \delta D_\mathrm{b}/G$, here δ is the grain-boundary thickness and G is the grain size,[15] the high densification rate should be due to the temperature of the grain boundary diffusion varying in an exponential manner.[16] Furthermore, high temperature sintering can reduce the yield stress of the ceramic particles and enhance the surface diffusion of atoms, which results in both the removal of the isolated pores and the higher densification.[16] Simultaneously, the grain coalescence and growth are inevitable in the heating-up and the densification process due to grain boundary migration and/or surface diffusion.[17] The average grain size of the sample S1548 is $\sim$ 0.5 μm, and a slight grain growth occurs with an increase in sintering temperature up to 1648 K (Figs. 3(b) and 3(c)). However, the average grain size increases from $\sim$ 0.7 μm to $\sim$ 7 μm (Figs. 3(c) and 3(d)) as the sintering temperature rises from 1648 K to 1748 K, showing significant grain growth at 1748 K. This situation suggests that the activation energy for grain growth is higher than that for densification in the case of Gd-doped STO, which is in agreement with the previously reported result concerning the non-doped STO ceramic.[18] However, a few nanoscale pores are located at the triple junctions of grain boundaries for the sample S1748 (Fig. 3(d)) in comparison to the case for sample S1648 (Fig. 3(c)). As a result, samples S1748 and S1648 are similar in relative density, indicating that the rapid grain growth caused by the high sintering temperature did not contribute to a further enhancement of densification.

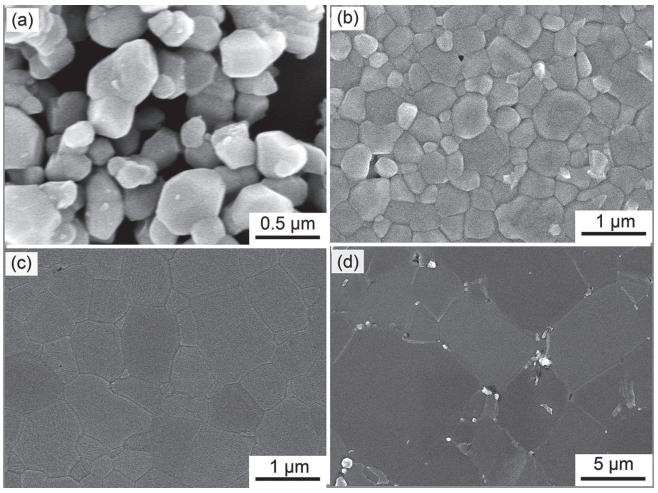


Fig. 3. SEM images of (a) SGTO powders, and the mirror-polished and thermal etched surfaces for (b) S1548, (c) S1648, and (d) S1748.

Figures 4(a) and 4(b) show the temperature dependences of electrical conductivity (σ) and Seebeck coefficient (S) for the samples SPSed at different temperatures. One can see that the values of σ for all the samples decrease monotonically and the absolute values of $|S|$ increase with increasing the temperature, indicating that the samples are degenerate semiconductors. In the whole temperature range, the negative values of S confirm that the major charge carriers in all the samples are electrons. The samples S1548 and S1648 almost have the same values of S (Fig. 4(b)), suggesting that the two samples have carrier concentration values close to each other.[19] Thus, an increase in σ is observed with SPS sintering temperature rising from 1548 K to 1648 K as shown in Fig. 4(a), which could be mainly ascribed to the increase of carrier mobility due to the enhanced densification and grown grains, according to the relationship between the electrical conductivity σ and the carrier mobility μ ($\sigma = ne\mu$).[20,21] Favored by the increase in σ as shown in Fig. 4(c), the PF is doubled at 300 K and increases from about 4 μW/K^2·cm to 7 μW/K^2·cm at 1000 K as the sintering temperature rises from 1548 K to 1648 K. Moreover, sample S1748 shows a smaller σ in value and a higher value of $|S|$ than sample S1648, which could be affected by the nanopores[13] or the different oxygen deficiencies.[22] This situation gives rise to the comparative values of PF between the two samples (Fig. 4(c)). The maximum PF values for samples S1548, S1648, and S1748 are about 7.2, 12.4, and 13.0 μW/K^2·cm, respectively. The higher PF value (12 μW/K^2·cm–13 μW/K^2·cm) should be ascribed to the dense microstructure with a relative density of higher than 98% and large grain size.

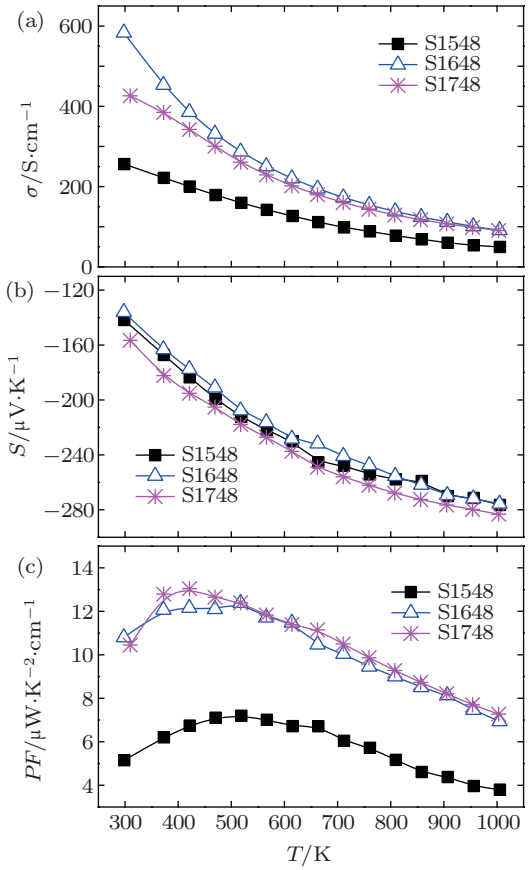


Fig. 4. (color online) Temperature dependences of (a) electrical conductivity, (b) Seebeck coefficient, and (c) power factor for S1548, S1648, and S1748.

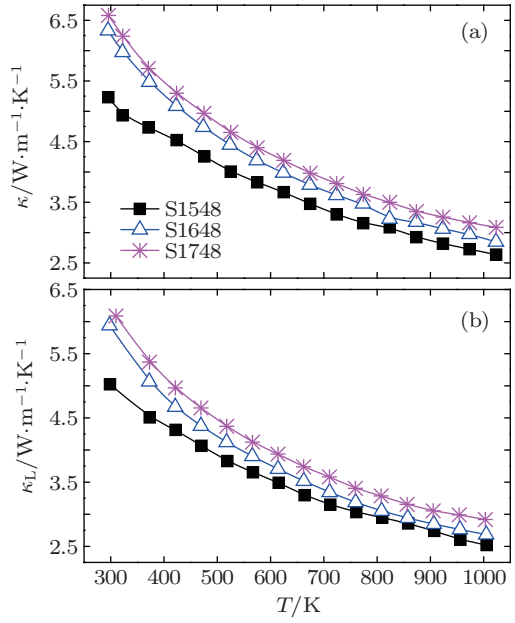


Fig. 5. (color online) Temperature dependences of (a) total thermal conductivity, and (b) lattice thermal conductivity for S1548, S1648, and S1748.

Plots of the total thermal conductivity (κ) versus temperature for all ceramic samples SPSed at different temperatures are presented in Fig. 5(a). The values of κ for SGTO samples basically increase with increasing the SPS temperature, especially in a range from 1548 K to 1648 K, i.e., the value of κ increases from $\sim$ 5.2 W/m·K to 6.6 W/m·K at room temperature and from 2.7 W/m·K to 2.9 W/m·K at $\sim$ 1000 K. Further increasing the sintering temperature up to 1748 K, the sample shows a slight increase in κ. In general, the κ is composed of the lattice thermal conductivity and the electronic thermal conductivity ($\kappa_L + \kappa_e$), where κ_e can be estimated by Wiedemann–Franz law: $\kappa_e = L_0 \sigma T$, with the Lorentz number L_0 taken to be 2.44×10^{-8} V^2/K^2. As shown in Fig. 5(b), κ_L is predominant in the total thermal conductivity. The increase in κ_L values for the samples SPSed at temperatures from 1548 K to 1748 K should be mainly ascribed to the decrease in the effect of phonon scattering at grain boundaries and/or pores, which is in line with the grain growth and densification.

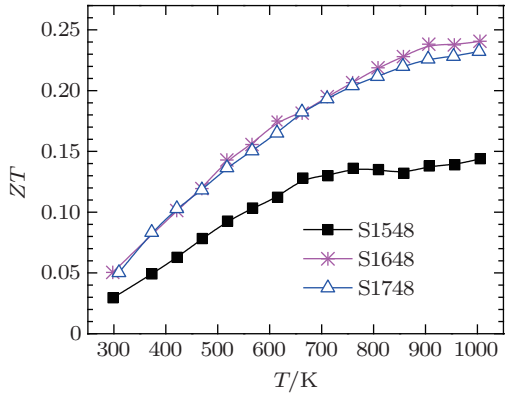


Fig. 6. (color online) Temperature dependence of the dimensionless figure of merit of three SGTO ceramics.

The temperature dependences of dimensionless figure of merit (ZT) for three samples are given in Fig. 6. Of the three samples, sample S1548 exhibits the lowest ZT value due to the relatively low σ, and the ZT value dramatically increases with sintering temperature rising from 1548 K to 1648 K. The maximum ZT of 0.24 is achieved at $\sim$ 1000 K for sample S1648, which is about 71% larger than that (0.14 at $\sim$ 1000 K) of sample S1548 in the present study. The enhancement of ZT value indicates that the ceramic fabricated by SPS with high densification not only improves PF but also maintains a reasonable κ value. Clearly, the peak ZT values for sample S1648 at high temperatures are comparable to that (0.27 at 1073 K) of the heavily La-doped STO single crystal,[23] but smaller than that (0.37 at 1073 K) of $Sr(Ti_{0.8}Nb_{0.2})O_3$ epitaxial film.[6] There is no obvious difference in the ZT value between S1648 and S1748 in the whole temperature range because of the comparative values of PF and κ. It can be concluded that the ZT value is affected feebly by sintering temperature as the SPS temperature rises over 1648 K. In conclusion, the densification of the microstructure is proven to be one of the most effective approaches to improving the TE performance of the STO-based oxide. Because the thermal conductivity is one of

the important factors for the better performance of STO-based oxide, further researches should be conducted for searching for the optimal composition and enhancing the ZT value by nano-inclusion.[21]

4. Conclusions

Single phase $(Sr_{0.95}Gd_{0.05})TiO_3$ powders are prepared by using a sol–gel method. After being annealed in the reducing atmosphere, the STGO powders are consolidated into ceramics by SPS at 1548, 1648, and 1748 K, respectively. As the SPS temperature increases from 1548 K to 1648 K, the relative densities of the ceramics dramatically increase, and the sample could be densified into a density of over 98% at a sintering temperature of 1648 K. The Seebeck coefficient is almost kept unchanged, but the electrical conductivity and thermal conductivity increase with increasing the SPS temperature, which should arise from the increased density and grain size. A maximum ZT of 0.24 is achieved at $\sim$ 1000 K for the sample SPSed at 1648 K, which is $\sim$71% larger than that (0.14 at $\sim$ 1000 K) for the sample SGTO SPSed at 1548 K. Further increasing the sintering temperature to 1748 K results in rapid growth of grain without enhancing densification, and the ZT value is almost unaffected by the sintering temperature due to the similar PF and κ values in the whole temperature range.

References

[1] DiSalvo F J 1999 *Science* **285** 703

[2] Zhang H, Luo J, Zhu H T, Liu Q L, Liang J K, Liu Q L, Liang J K, Li J B and Liu G Y 2012 *Chin. Phys. B* **21** 106101

[3] Zou T H, Qin X Y, Li D, Ren B J, Sun G L, Dou Y C, Li Y Y, Li L L, Zhang J and Xin H X 2014 *J. Appl. Phys.* **115** 053710

[4] Koumoto K, Wang Y F, Zhang R Z, Kosuga A and Funahashi R 2010 *Ann. Rev. Mater. Res.* **40** 363

[5] Guo H H, Yang T, Tao P and Zhang Z D 2014 *Chin. Phys. B* **23** 017201

[6] Ohta S and Nomura T 2005 *Appl. Phys. Lett.* **87** 092108

[7] Kovalevsky A V, Yaremchenko A A, Populoh S, Weidenkaff A and Frade J R 2013 *J. Appl. Phys.* **113** 053704

[8] Muta H, Kurosaki K and Yamanaka S 2003 *J. Alloys Compd.* **350** 292

[9] Wang S F, Yan G Y, Chen S S, Bai Z L, Wang J L, Yu W and Fu G S 2013 *Chin. Phys. B* **22** 037302

[10] Perillat-Merceroz C, Gauthier G, Roussel P, Huve M, Gelin P and Vannier R 2011 *Chem. Mater.* **23** 1539

[11] Shang P P, Zhang B P, Li J F and Ma N 2010 *Solid State Sci.* **12** 1341

[12] Ravichandran J, Siemons W, Oh D W, Kardel J T, Chari A, Heijmerikx H, Scullin M L, Majumdar A, Ramesh R and Cahill D G 2010 *Phys. Rev. B* **82** 165126

[13] Lee H, Vashaee D, Wang D Z, Dresselhaus M S, Ren Z F and Chen G 2010 *J. Appl. Phys.* **107** 094308

[14] Chaim R and Margulis M 2005 *Mater. Sci. Eng. A* **407** 180

[15] Chen I W and Wang X H 2000 *Nature* **404** 168

[16] Chaim R, Marder R, Estournes C and Shen Z 2012 *Adv. Appl. Ceram.* **111** 280

[17] Hu J and Shen Z 2012 *Acta Mater.* **60** 6405

[18] Baurer M, Weygand D, Gumbsch P and Hoffmann M J 2009 *Scr. Mater.* **61** 584

[19] Moos R, Gnudi A and Hardtl K H 1995 *J. Appl. Phys.* **78** 5042

[20] Cui Y J, He J, Amow G and Kleinke H 2010 *Dalton Trans.* **39** 1031

[21] Wang N, Chen H J, He H C, Norimatsu W, Kusunoki M and Koumoto K 2013 *Sci. Rep.* **3** 3449

[22] Liu J, Wang C L, Su W B, Wang H C, Zheng P, Li J C, Zhang J L and Mei L M 2009 *Appl. Phys. Lett.* **95** 162110

[23] Ohta S, Nomura T, Ohta H and Koumoto K 2005 *J. Appl. Phys.* **97** 034106